Integrated Robust Control of Individual Scalar Variables in Tokamaks

Andres Pajares and Eugenio Schuster

***Abstract*— Tokamaks are devices with a toroidal shape in which a high-temperature ionized gas (plasma) is confined by means of helical magnetic fields. The final goal of these devices is to obtain energy from thermonuclear fusion reactions within this plasma. A multitude of coupled control problems arise in tokamak-plasma research that need to be solved simultaneously. For tokamaks to be able to operate safely while maximizing plasma performance, integrated control schemes that can handle different aspects of the plasma dynamics must be developed. Moreover, due to the inherent uncertainty that exists in the plasma modeling process, such controllers must be robust against unknown variations of the plasma behavior. In this work, a nonlinear, robust controller is designed for simultaneous regulation of magnetic and kinetic scalar variables, namely the central safety factor, q_0, the edge safety factor, q_{edge}, the total stored energy, W, and the global toroidal rotation, Ω_ϕ. The controller is synthesized from physics-based, zero-dimensional (0D) models of the individual scalars' dynamics. One-dimensional (1D) simulations using the COTSIM (Control-Oriented Transport Simulator) code are employed to test the proposed controller in a DIII-D scenario.**

I. Introduction

Tokamaks magnetically confine a plasma composed of hydrogen isotopes (normally deuterium, and most likely a mix of deuterium and tritium in the future). In order to obtain energy from nuclear fusion reactions, the triple product of the plasma density, temperature, and confinement time must be high enough [1]. To achieve a stable plasma, tokamak magnetic-field lines are twisted and form helical lines as depicted in Fig. 1. Whereas the toroidal component of the magnetic field, B_ϕ, is generated by the toroidal field coils and is approximately constant in time, the poloidal magnetic field, B_θ, is mainly due to the electrical current that is driven through the plasma using a transformer principle [1]. The plasma current ohmically heats the plasma and increases its temperature. However, such ohmic heating is only effective when the plasma is "cold" in the initial stages of the plasma discharge, because the plasma resistivity decreases when the plasma temperature increases. To further heat the plasma, additional auxiliary sources are employed. Two of the most used and well-known non-inductive auxiliary heating and current drive (H&CD) methods are neutral beam injection (NBI) and electron-cyclotron (EC) resonance.

Three plasma properties that are of interest in tokamak research are the plasma thermal energy-density profile, denoted by E, the toroidal rotation profile, ω_ϕ, and the safety factor profile, q, which is a measure of the pitch of the magnetic-field lines. Because E is directly proportional to the electron and ion temperatures, and to the electron and ion densities, it is desired that E is as high as possible for long periods of time (so that the triple product of density, temperature and confinement time is as high as possible too). Moreover, both ω_ϕ and q have a close relationship with the plasma confinement properties. For example, some particular q-profile shapes promote the development of internal transport barriers, which improve the plasma confinement. Also, high ω_ϕ profiles may also create internal transport barriers. In addition, numerous magneto-hydrodynamic (MHD) instabilities, which decrease plasma confinement and may terminate the plasma discharge, are related with E, ω_ϕ, and q. For instance, $q > 1$ avoids the so-called sawtooth instability, whereas ω_ϕ is closely related to the locking of neoclassical tearing modes and the development of resistive wall modes.

As a result, active control of E, ω_ϕ and/or q are problems of interest in nuclear fusion research. Nonetheless, simultaneous control of all these profiles is a great challenge due to the limited actuation capability existing in a tokamak. Instead, simultaneous control of a particular set of scalar magnitudes (such as some global magnitudes related to certain profiles, or particular values of a given profile at specific points) may fulfill the control requirements in future reactor-grade tokamaks, and represents a more attainable control problem. In this work, the central safety factor, q_0, edge safety factor, q_{edge}, global toroidal rotation, Ω_ϕ, and stored thermal energy, W, compose the set of scalars of interest for control.

To the authors knowledge, there is no previous work on integrated control of individual scalars related to energy, rotation, and safety factor simultaneoulsy. Previous work on simultaneous rotation (either ω_ϕ or Ω_ϕ) and W control can be found in [2], [3], [4], whereas work on simultaneous energy (either W, normalized beta, β_N, or electron temperature, T_e) and q-profile control can be found in [5], [6], [7], [8]. In this work, a fully-nonlinear, coupled model of the q_0, q_{edge}, W and Ω_ϕ dynamics is employed to synthesize a controller for these individual scalars. Moreover, uncertainties are included in the modeling process to account for unknown and/or unmodeled dynamics. Nonlinear, robust controllers involving Lyapunov redesign techniques are employed to handle such uncertainties. The actuators considered are the NBI and EC powers, and the plasma current.

This work is organized as follows. The model for the individual-scalars dynamics is given in Section II. The controller is designed in Section III. A 1D-simulation study to test the controller in a DIII-D scenario is included in Section IV. Finally, some conclusions and possible future work are suggested in Section V.

This work was supported in part by the U.S. Department of Energy (DE-SC0010661). A. Pajares (andres.pajares@lehigh.edu) and E. Schuster are with the Department of Mechanical Engineering and Mechanics, Lehigh University, Bethlehem, PA 18015, USA.

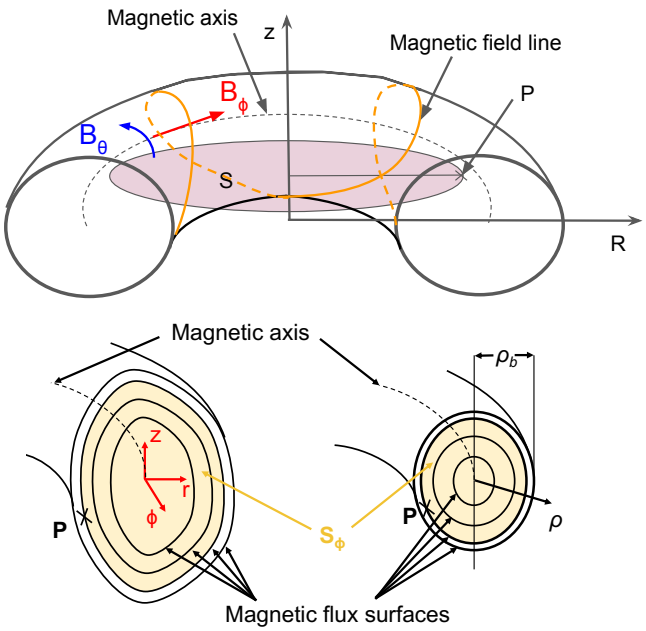

Fig. 1. Magnetic configuration in a tokamak.

II. Dynamics of Zero-Dimensional Plasma Variables

Under ideal MHD conditions, the magnetic-flux surfaces in a tokamak form toroidally nested surfaces around the magnetic axis (see Fig. 1). A magnetic-flux surface is defined by points with the same value of the toroidal magnetic flux, Φ, mean effective minor radius, ρ, poloidal magnetic flux, Ψ, pressure p, or others [1]. Only one of these functions (known as flux functions) is needed to index the magnetic-flux surfaces. This, together with the assumption of toroidal symmetry, reduces the 3D-problem in space to a 1D-problem.

At a point P, the toroidal magnetic flux is defined as $\Phi = \int_{S_\phi} B_\phi dS_\phi$, where S_ϕ is the surface enclosed by the magnetic-flux surface that passes through P and is normal to the ϕ axis, as depicted in Fig. 1. The mean effective minor radius, ρ, is defined as $\Phi = B_{\phi,0}\pi\rho^2$, where $B_{\phi,0}$ is the vacuum toroidal magnetic field at the major radius, R_0. A non-dimensional version of ρ is given by $\hat{\rho} \triangleq \rho/\rho_b$, where ρ_b is the mean effective minor radius of the last-closed magnetic-flux surface. Analogously to the toroidal flux Φ, the poloidal magnetic flux at a point P is defined as $\Psi = \int_S B_\theta dS$, where S is the surface whose boundary is a toroidal ring that passes through P and is normal to the z axis, as depicted in Fig. 1. The poloidal stream function, ψ, is given by $\psi = \Psi/(2\pi)$. The safety factor, q, is defined as

$$q \triangleq -\frac{d\Phi}{d\Psi} = -\frac{B_{\phi,0}\rho_b^2\hat{\rho}}{\partial\psi/\partial\hat{\rho}}. \tag{1}$$

The pressure field, p, is given by

$$p = n_e K T_e + n_i K T_i, \tag{2}$$

where n_e and n_i are the electron and ion densities, respectively, T_e and T_i are the electron and ion temperatures, respectively, and K is the Boltzmann's constant. It is assumed that the plasma is quasi-neutral and purely hydrogenic, $n_e \approx n_i \triangleq n$, so (2) becomes $p = nK(T_e + T_i)$. The thermal energy-density, E, is given by $E = \frac{3}{2}nK(T_e+T_i) = \frac{3}{2}p$, so E is a constant in a magnetic-flux surface as well.

A. Central Safety Factor

The central safety factor, q_0, is the value of q at $\hat{\rho} = 0$,

$$q_0(t) \triangleq -\left.\frac{B_{\phi,0}\rho_b^2\hat{\rho}}{\partial\psi(\hat{\rho},t)/\partial\hat{\rho}}\right|_{\hat{\rho}=0} = -\left.\frac{B_{\phi,0}\rho_b^2}{\partial\theta(\hat{\rho},t)/\partial\hat{\rho}}\right|_{\hat{\rho}=0}, \tag{3}$$

where $\theta \triangleq \partial\psi/\partial\hat{\rho}$, and L'Hopital's rule has been employed. If $\partial\theta(\hat{\rho},t)/\partial\hat{\rho}|_{\hat{\rho}=0} \approx \theta(\Delta\hat{\rho},t)/\Delta\hat{\rho}$, where $\Delta\hat{\rho}$ is a small parameter, then

$$q_0(t) \triangleq -\left.\frac{B_{\phi,0}\rho_b^2\hat{\rho}}{\partial\psi(\hat{\rho},t)/\partial\hat{\rho}}\right|_{\hat{\rho}=0} \approx -\frac{B_{\phi,0}\rho_b^2\Delta\hat{\rho}}{\theta(\Delta\hat{\rho},t)}, \tag{4}$$

and taking time derivative, it is found that

$$\frac{dq_0}{dt} \approx \frac{B_{\phi,0}\rho_b^2\Delta\hat{\rho}}{\theta(\Delta\hat{\rho},t)^2}\,\frac{d\theta(\Delta\hat{\rho},t)}{dt}, \tag{5}$$

so the dynamics of q_0 is in fact defined by the dynamics of $\theta(\Delta\hat{\rho})$ using this approximation. The dynamics of ψ and θ is defined by the magnetic diffusion equation (MDE) [9],

$$\frac{\partial\psi}{\partial t} = \frac{\eta}{\mu_0\rho_b^2\hat{F}^2}\frac{1}{\hat{\rho}}\frac{\partial}{\partial\hat{\rho}}\left(\hat{\rho}D_\psi\frac{\partial\psi}{\partial\hat{\rho}}\right) + R_0\hat{H}\eta j_{ni}, \tag{6}$$

$$\left.\frac{\partial\psi}{\partial\hat{\rho}}\right|_{\hat{\rho}=0} = 0, \qquad \left.\frac{\partial\psi}{\partial\hat{\rho}}\right|_{\hat{\rho}=1} = -\frac{\mu_0}{2\pi}\frac{R_0}{\hat{G}|_{\hat{\rho}=1}\hat{H}|_{\hat{\rho}=1}}I_p, \tag{7}$$

where η is the plasma resistivity, j_{ni} is the non-inductive current, and $\hat{F}$, $\hat{G}$, $\hat{H}$, $D_\psi \triangleq \hat{F}\hat{G}\hat{H}$ are profiles corresponding to a particular magnetic configuration, μ_0 is the vacuum magnetic permeability, and I_p is the plasma current. Following the same ideas and control-oriented models for T_e, n_e, η, and j_{ni} as in [10], (6) can be written as

$$\begin{aligned}\frac{\partial\theta}{\partial t} = &\left(h_{diff,1}\frac{\partial^2\theta}{\partial\hat{\rho}^2} + h_{diff,2}\frac{\partial\theta}{\partial\hat{\rho}} + h_{diff,3}\theta\right)u_\eta^{virt} \\ &+ \sum_{i=1}^{N_{NBI}} h_{NBI,i}u_{NBI,i}^{virt} + h_{EC}u_{EC}^{virt} \\ &+ \left(h_{BS,1}\frac{1}{\theta} - h_{BS,2}\frac{\theta}{\partial\theta/\partial\hat{\rho}}\right)u_{BS}^{virt},\end{aligned} \tag{8}$$

where $h_{(\cdot)}$ are spatial functions that depend only on $\hat{\rho}$, and $u_{(\cdot)}^{virt}$ are the "virtual inputs" to the system, which are functions of the physical inputs, namely, I_p, the power of the i-th NBI, $P_{NBI,i}$ ($i = 1, ..., N_{NBI}$, where N_{NBI} is the total number of NBI's), the total EC power, P_{EC}, and the line-average electron density, $\bar{n}_e$, as given by

$$u_\eta^{virt} = (I_p^\gamma P_{tot}^\epsilon \bar{n}_e^\zeta)^{-3/2}, \tag{9}$$

$$u_{NBI,i}^{virt} = (I_p^\gamma P_{tot}^\epsilon \bar{n}_e^\zeta)^{(-3/2+\xi_{NBI})}\bar{n}_e^{-1}P_{NBI,i}, \tag{10}$$

$$u_{EC}^{virt} = (I_p^\gamma P_{tot}^\epsilon \bar{n}_e^\zeta)^{(-3/2+\xi_{EC})}\bar{n}_e^{-1}P_{EC}, \tag{11}$$

$$u_{BS}^{virt} = (I_p^\gamma P_{tot}^\epsilon \bar{n}_e^\zeta)^{-3/2}\bar{n}_e, \tag{12}$$

where γ, ϵ, ζ, ξ_{NBI} and ξ_{EC} are model parameters, and P_{tot} is the total injected power, $P_{tot} = \sum_{i=1}^{N_{NBI}} P_{NBI,i} + P_{EC}$.

By evaluating (8) at $\hat{\rho}=0$ with its first spatial derivative $\partial\theta/\partial\hat{\rho}|_{\hat{\rho}=0}$ discretized as in (4) and its second spatial derivative discretized as $\partial^2\theta/\partial\hat{\rho}^2|_{\hat{\rho}=0} \approx (\theta(2\Delta\hat{\rho})-2\theta(\Delta\hat{\rho}))/\Delta\hat{\rho}^2$, and using (4), the dynamics for q_0 (5) can be rewritten as

$$\begin{aligned}\frac{dq_0}{dt} &= q_0\left(\lambda_{diff,1}+\lambda_{diff,2}\frac{\theta(2\Delta\hat{\rho})}{\theta(\Delta\hat{\rho})}\right)u_\eta^{virt}\\ &+ q_0^2\left(\sum_{i=1}^{N_{NBI}}\lambda_{NBI,i}u_{NBI,i}^{virt}+\lambda_{EC}u_{EC}^{virt}\right)\\ &- q_0^3\left(\lambda_{BS,1}-\lambda_{BS,2}\frac{\theta(2\Delta\hat{\rho})}{\theta(\Delta\hat{\rho})}\right)u_{BS}^{virt},\end{aligned} \tag{13}$$

where $\lambda_{(\cdot)}$ are constant model parameters derived from $h_{(\cdot)}$. It is assumed that $\theta(2\Delta\hat{\rho})/\theta(\Delta\hat{\rho})$ is uncertain and given by $\frac{\theta(2\Delta\hat{\rho})}{\theta(\Delta\hat{\rho})} = \frac{\theta(2\Delta\hat{\rho})}{\theta(\Delta\hat{\rho})}\Big|_{nom}+\delta_\theta$, where $\theta(2\Delta\hat{\rho})/\theta(\Delta\hat{\rho})|_{nom}$ is a nominal, known value, and δ_θ is an uncertain term. This assumption not only implies that the influence of the rest of the q-profile evolution on q_0 is taken as uncertain, but also enables modeling of any other source of unknown dynamics (e.g., uncertainties in T_e, that affects η and j_{ni} in (6), see [10]). Then, (13) is written as

$$\begin{aligned}\frac{dq_0}{dt} &= q_0\left(\lambda_{diff,1}+\lambda_{diff,2}\left.\frac{\theta(2\Delta\hat{\rho})}{\theta(\Delta\hat{\rho})}\right|_{nom}\right)u_\eta^{virt}\\ &+ q_0^2\left(\sum_{i=1}^{N_{NBI}}\lambda_{NBI,i}u_{NBI,i}^{virt}+\lambda_{EC}u_{EC}^{virt}\right)\\ &- q_0^3\left(\lambda_{BS,1}+\lambda_{BS,2}\left.\frac{\theta(2\Delta\hat{\rho})}{\theta(\Delta\hat{\rho})}\right|_{nom}\right)u_{BS}^{virt}+\delta_{q_0},\end{aligned} \tag{14}$$

where $\delta_{q_0}=(q_0\lambda_{diff,2}u_\eta^{virt}+q_0^3\lambda_{BS,2}u_{BS}^{virt})\delta_\theta$ is a term that bundles the uncertainties in the q_0 subsystem.

B. Edge Safety Factor

The edge safety factor, q_{edge}, is the value of q at $\hat{\rho}=1$. Its dynamics can be obtained by taking time derivative in the MDE boundary condition at $\hat{\rho}=1$ (second equation in (7)),

$$\frac{dq_{edge}}{dt} = -\frac{B_{\phi,0}\rho_b^2}{k_{I_p}I_p^2}\frac{dI_p}{dt}, \tag{15}$$

where $k_{I_p} \triangleq \mu_0 R_0/(2\pi\hat{G}|_{\hat{\rho}=1}\hat{H}|_{\hat{\rho}=1}) > 0$ is a model parameter. It is taken as $k_{I_p}=k_{I_p}^{nom}+\delta_{k_{I_p}}$, where $k_{I_p}^{nom}$ is a constant, known value of k_{I_p}, and $\delta_{k_{I_p}}$ is an uncertain term, representing unknown variations in the plasma magnetic configuration and position.

C. Thermal Stored Energy

The thermal stored energy, W, is defined as

$$W(t) \triangleq \int_{V_p} E\,dV = \int_{\hat{\rho}=0}^{\hat{\rho}=1} E(\hat{\rho},t)\frac{\partial V(\hat{\rho},t)}{\partial\hat{\rho}}d\hat{\rho}, \tag{16}$$

where V_p is the plasma region enclosed within the last magnetic-flux surface, and $V(\hat{\rho})$ is the plasma volume enclosed by the magnetic-flux surface labeled with $\hat{\rho}$.

The dynamics of W is modeled using a 0D energy balance,

$$\frac{dW}{dt} = -\frac{W}{\tau_E}+P_{tot}+\delta_W, \tag{17}$$

where $\tau_E = H_H^{nom}kI_p^{0.93}{P_{tot}}^{-0.69}$ is the energy confinement time, which is modeled using the IPB98(y,2) scaling [11], k is a constant that depends on the machine parameters ($B_{\phi,0}$, R_0, etc.), H_H^{nom} is the nominal H factor, and $\delta_W = \frac{W}{kI_p^{0.93}{P_{tot}}^{-0.69}}(\frac{1}{H_H^{nom}}-\frac{1}{H_H})+\delta_P$ is a term that bundles all the uncertain terms of the W-subsystem [12].

D. Global Toroidal Rotation

The global toroidal rotation, Ω_ϕ, is defined as the average toroidal rotation of the ions inside the plasma, and it is given by

$$\Omega_\phi(t) \triangleq \frac{1}{N_p(t)}\int_{V_p} n(\hat{\rho},t)\,\omega_\phi(\hat{\rho},t)dV, \tag{18}$$

where N_p is the total number of ions within the plasma.

The dynamics of Ω_ϕ is modeled using a 0D toroidal momentum balance,

$$\begin{aligned}\frac{d\Omega_\phi}{dt} &= -\frac{\Omega_\phi}{k_\Omega H_H^{nom}k{P_{tot}}^{-0.69}}\\ &+ \sum_{i=1}^{N_{NBI}}\frac{k_{NBI,i}P_{NBI,i}}{m_pR_0^2}+k_{int}\frac{W}{I_pm_pR_0^2}+\delta_\Omega,\end{aligned} \tag{19}$$

where k_Ω, $k_{NBI,i}$ and k_{int} are model constants, m_p is the mass of the plasma confined within the last-closed magnetic-flux surface, and $\delta_\Omega = \frac{\Omega_\phi}{k_\Omega k{P_{tot}}^{-0.69}}(\frac{1}{H_H^{nom}}-\frac{1}{H_H})+\delta_T$ is a term that bundles all the uncertain terms of the Ω_ϕ-subsystem [12].

E. Summary: State-Space Model

The state-space model for the system is given by $\dot{x}=f(x,u,t,\delta)$, where $x=[q_0,q_{edge},W,\Omega_\phi]^T$ is the state, $u=[I_p,P_{NBI,1},...,P_{NBI,N_{NBI}}]^T$ is the controllable input, $\delta=[\delta_{q_0},\delta_{k_{I_p}},\delta_W,\delta_\Omega]^T$ is the uncertainty, and $f=[f_{q_0},f_{q_{edge}},f_W,f_{\Omega_\phi}]^T\in\mathbb{R}^{4\times1}$, where f_{q_0}, $f_{q_{edge}}$, f_W, and f_{Ω_ϕ} are given by the right hand side of (14), (15), (17), and (19), respectively. The explicit dependence with t is due to $\bar{n}_e$ and m_p, which are non-controllable in this work.

III. Control Design

The control objective is to drive x to a target value, $\bar{x}$. The control algorithm is composed of 4 controllers (one for each individual scalar). Each controller generates one constraint for the $N_{NBI}+2$ components of u. In order to obtain u at each time step, the constraints are embedded into an optimization problem together with the saturation limits.

A. q_{edge} control by means of I_p

The first step is to control q_{edge} by means of I_p. It is convenient to employ θ at the edge, $\theta_N=-B_{\phi,0}\rho_b^2/q_{edge}$, instead of q_{edge}, because its dependence with I_p and k_{I_p} is linear ($\theta_N=-k_{I_p}I_p$). Because dI_p/dt is present in (15), it is discretized for control purposes as $dI_p/dt \approx (I_p(t)-I_p(t-\Delta t))/\Delta t$, where Δt is the controller sampling time. First, the nominal system ($\delta_{k_{I_p}}=0$) is considered to look for a nominal control law I_p^{nom}. As $k_{I_p}^{nom}$ is a constant, (15) can be rewritten in terms of θ_N as

$$\frac{d\theta_N}{dt} = -k_{I_p}^{nom}\frac{I_p^{nom}(t)-I_p(t-\Delta t)}{\Delta t} \triangleq f_{\theta_N}(I_p^{nom}). \tag{20}$$

By setting (20) as

$$f_{\theta_N}(I_p^{nom}) \equiv -k_{P,\theta_N}\tilde{\theta}_N - k_{I,\theta_N}\int_{t_0}^{t}\tilde{\theta}_N dt + \frac{d\bar{\theta}_N}{dt}, \quad (21)$$

where $\bar{\theta}_N$ is the target for θ_N (related to $\bar{q}_{edge}$ by $\bar{\theta}_N = -B_{\phi,0}\rho_b^2/\bar{q}_{edge}$), $\tilde{\theta}_N \triangleq \theta_N - \bar{\theta}_N$, and $k_{P,\theta_N} > 0$, $k_{I,\theta_N} > 0$ are design parameters, the θ_N-dynamics becomes $d\tilde{\theta}_N/dt = -(k_{P,\theta_N}\tilde{\theta}_N + k_{I,\theta_N}\int_{t_0}^{t}\tilde{\theta}_N dt)$. The nominal control law obtained from (21) ensures $\tilde{\theta}_N \to 0$ for the nominal θ_N-subsystem [13]. To ensure robustness under $\delta_{k_{I_p}} \neq 0$, a term I_p^{rob} is added to I_p^{nom}, so that the final control law is $I_p = I_p^{nom} + I_p^{rob}$. Equation (20) can be rewritten in the uncertain case as

$$\frac{d\tilde{\theta}_N}{dt} = k_{I_p}^{nom}\frac{I_p(t-\Delta t)}{\Delta t} - \frac{d\bar{\theta}_N}{dt} - \frac{k_{I_p}^{nom}}{\Delta t}(I_p + \delta_{\theta_N}), \quad (22)$$

where $\delta_{\theta_N} = (I_p - I_p(t-\Delta t))\delta_{k_{I_p}}/k_{I_p}^{nom}$ is a term that bundles all the uncertain terms of the θ_N-subsystem, and for which it is assumed that a bound, $\delta_{\theta_N}^{max}$, can be estimated. Using Lyapunov redesign techniques [13], it can be shown that a stabilizing control law for I_p^{rob} is given by

$$I_p^{rob} = K_{R,\theta_N}\,\text{sign}(\tilde{\theta}_N), \qquad \text{if } \delta_{\theta_N}^{max}|\tilde{\theta}_N| \geq \epsilon_{\theta_N}, \quad (23)$$
$$I_p^{rob} = K_{R,\theta_N}^2\tilde{\theta}_N/\epsilon_{\theta_N}, \qquad \text{if } \delta_{\theta_N}^{max}|\tilde{\theta}_N| < \epsilon_{\theta_N}, \quad (24)$$

where $K_{R,\theta_N} \geq \delta_{\theta_N}^{max}$ and $\epsilon_{\theta_N} \to 0$ are design parameters.

B. W control by means of P_{tot}

The second step is to control W by means of P_{tot}. In this step and the subsequent steps, the value of I_p is fixed and given by (21) and (23)-(24). To look for a nominal control law P_{tot}^{nom}, equation (17) with $\delta_W = 0$ is set as

$$f_W(x, P_{tot}^{nom}, t, 0) = -\frac{\bar{W}+\tilde{W}}{H_H^{nom}kI_p^{0.93}P_{tot}^{nom\,-0.69}} + P_{tot}^{nom}$$
$$\equiv -k_{P,W}\tilde{W} - k_{I,W}\int_{t_0}^{t}\tilde{W}dt + \frac{d\bar{W}}{dt}, \quad (25)$$

where $\tilde{W} \triangleq W - \bar{W}$, and $k_{P,W} > 0$ and $k_{I,W} > 0$, the W-dynamics becomes $d\tilde{W}/dt = -(k_{P,W}\tilde{W} + k_{I,W}\int_{t_0}^{t}\tilde{W}dt)$. The nominal control law obtained from (25) ensures $\tilde{W} \to 0$ for the nominal W-subsystem. To ensure robustness under $\delta_W \neq 0$, a term P_{tot}^{rob} is added to P_{tot}^{nom} so that the final control law is $P_{tot} = P_{tot}^{nom} + P_{tot}^{rob}$. Assuming that a bound to δ_W is known, δ_W^{max}, it can be shown [13] that a stabilizing control law for $u_P^{rob} \triangleq P_{tot}^{rob} - \frac{\bar{W}+\tilde{W}}{H_H^{nom}kI_p^{0.93}P_{tot}^{rob}}$ is given by

$$u_P^{rob} = K_{R,W}\,\text{sign}(\tilde{W}), \qquad \text{if } \delta_W^{max}|\tilde{W}| \geq \epsilon_W, \quad (26)$$
$$u_P^{rob} = K_{R,W}^2\tilde{W}/\epsilon_W, \qquad \text{if } \delta_W^{max}|\tilde{W}| < \epsilon_W, \quad (27)$$

where $K_{R,W} \geq \delta_W^{max}$ and $\epsilon_W \to 0$ are design parameters.

C. Ω_ϕ control by means of $\sum_i T_{NBI,i}$

The third step is to control Ω_ϕ by means of $T_{NBI} \triangleq \sum_i k_{NBI,i}P_{NBI,i}$. In this step and the subsequent steps, the value of P_{tot} is fixed (as well as I_p) and given by (25) and (26)-(27). To look for a nominal control law T_{NBI}^{nom}, equation (19) with $\delta_\Omega = 0$ is set as

$$f_\Omega(x, T_{NBI}^{nom}, t, 0) = -\frac{\bar{\Omega}_\phi + \tilde{\Omega}_\phi}{k_\Omega H_H^{nom}kP_{tot}^{-0.69}} + \frac{T_{NBI}^{nom}}{m_pR_0^2}$$
$$+ k_{int}\frac{\bar{W}+\tilde{W}}{I_p m_p R_0^2} \equiv -k_{P,\Omega}\tilde{\Omega}_\phi - k_{I,\Omega}\int_{t_0}^{t}\tilde{\Omega}_\phi dt + \frac{d\bar{\Omega}_\phi}{dt}, \quad (28)$$

where $\tilde{\Omega}_\phi \triangleq \Omega_\phi - \bar{\Omega}_\phi$, and $k_{P,\Omega} > 0$ and $k_{I,\Omega} > 0$, the Ω_ϕ-dynamics becomes $d\tilde{\Omega}_\phi/dt = -(k_{P,\Omega_\phi}\tilde{\Omega}_\phi + k_{I,\Omega_\phi}\int_{t_0}^{t}\tilde{\Omega}_\phi dt)$. The nominal control law obtained from (28) ensures $\tilde{\Omega}_\phi \to 0$ for the nominal Ω_ϕ-subsystem. To ensure robustness under $\delta_\Omega \neq 0$, a term T_{NBI}^{rob} is added to T_{NBI}^{nom}, so that the final control law is $T_{NBI} = T_{NBI}^{nom} + T_{NBI}^{rob}$. Assuming that a bound to δ_Ω is known, δ_Ω^{max}, it can be shown [13] that a stabilizing control law for $T_{NBI,i}^{rob}$ is given by

$$T_{NBI,i}^{rob} = -K_{R,\Omega}\,\text{sign}(\tilde{\Omega}_\phi), \qquad \text{if } \delta_\Omega^{max}|\tilde{\Omega}_\phi| \geq \epsilon_\Omega, \quad (29)$$
$$T_{NBI,i}^{rob} = -K_{R,\Omega}^2\tilde{\Omega}_\phi/\epsilon_\Omega, \qquad \text{if } \delta_\Omega^{max}|\tilde{\Omega}_\phi| < \epsilon_\Omega, \quad (30)$$

where $K_{R,\Omega} \geq \max|\delta_\Omega|$ and $\epsilon_\Omega \to 0$ are design parameters.

D. q_0 control by means of $P_{NBI,i}$ and P_{EC}

The fourth step is to control q_0 by means of $P_{NBI,i}$ and P_{EC}. By setting (14) with $\delta_{q_0} = 0$ as

$$f_{q_0}(x, u^{nom}, t, 0) \equiv -k_{P,q_0}\tilde{q}_0 - k_{I,q_0}\int_{t_0}^{t}\tilde{q}_0 dt + \frac{d\bar{q}_0}{dt}, \quad (31)$$

where $\tilde{q}_0 \triangleq q_0 - \bar{q}_0$, and $k_{P,q_0} > 0$ and $k_{I,q_0} > 0$, the q_0-dynamics becomes $d\tilde{q}_0/dt = -(k_{P,q_0}\tilde{q}_0 + k_{I,q_0}\int_{t_0}^{t}\tilde{q}_0 dt)$. The nominal control law obtained from (31) ensures $\tilde{q}_0 \to 0$ for the nominal q_0-subsystem. It can be noted that (31) is in fact a constraint for $P_{NBI,i}$ and P_{EC} only (u_η^{virt} and u_{BS}^{virt} are already determined because I_p, P_{tot} and $\bar{n}_e$ are determined, see equations (9)-(12)), and it can be rewritten as

$$q_0^2 F P^{nom} \equiv -k_{P,q_0}\tilde{q}_0 - k_{I,q_0}\int_{t_0}^{t}\tilde{q}_0 dt + \frac{d\bar{q}_0}{dt}$$
$$- q_0\left(\lambda_{diff,1} + \lambda_{diff,2}\left.\frac{\theta(2\Delta\hat{\rho})}{\theta(\Delta\hat{\rho})}\right|_{nom}\right)u_\eta^{virt}$$
$$+ q_0^3\left(\lambda_{BS,1} + \lambda_{BS,2}\left.\frac{\theta(2\Delta\hat{\rho})}{\theta(\Delta\hat{\rho})}\right|_{nom}\right)u_{BS}^{virt}, \quad (32)$$

where $F \in \mathbb{R}^{1\times N_{NBI}+1}$ is a vector whose i-th component is given by (see equations (9)-(12)) $\lambda_{NBI,i}(I_p^\gamma P_{tot}^\epsilon \bar{n}_e^\zeta)^{(-3/2+\xi_{NBI})}\bar{n}_e^{-1}$, except for the last one, which is given by $\lambda_{EC}(I_p^\gamma P_{tot}^\epsilon \bar{n}_e^\zeta)^{(-3/2+\xi_{EC})}\bar{n}_e^{-1}$, and $P^{nom} = [P_{NBI,1}^{nom}, ..., P_{NBI,N_{NBI}}^{nom}, P_{EC}^{nom}]^T$ is a vector with the nominal NBI and EC powers. To ensure robustness under $\delta_{q_0} \neq 0$, a term $P^{rob} = [P_{NBI,1}^{rob}, ..., P_{NBI,1}^{rob}, P_{EC}^{rob}]^T$ is added to P^{nom}, so that the final control law is $P = P^{nom} + P^{rob}$. If a bound to δ_{q_0} is known (denoted by $\delta_{q_0}^{max}$), the robust term P^{rob} is computed by [13]

$$FP^{rob} = -K_{R,q_0}\,\text{sign}(\tilde{q}_0), \qquad \text{if } \delta_{q_0}^{max}|\tilde{q}_0| \geq \epsilon_{q_0}, \quad (33)$$
$$FP^{rob} = -K_{R,q_0}^2\tilde{q}_0/\epsilon_{q_0}, \qquad \text{if } \delta_{q_0}^{max}|\tilde{q}_0| < \epsilon_{q_0}, \quad (34)$$

where $K_{R,W} \geq \delta_{q_0}^{max}$ and $\epsilon_{q_0} \to 0$ are design parameters.

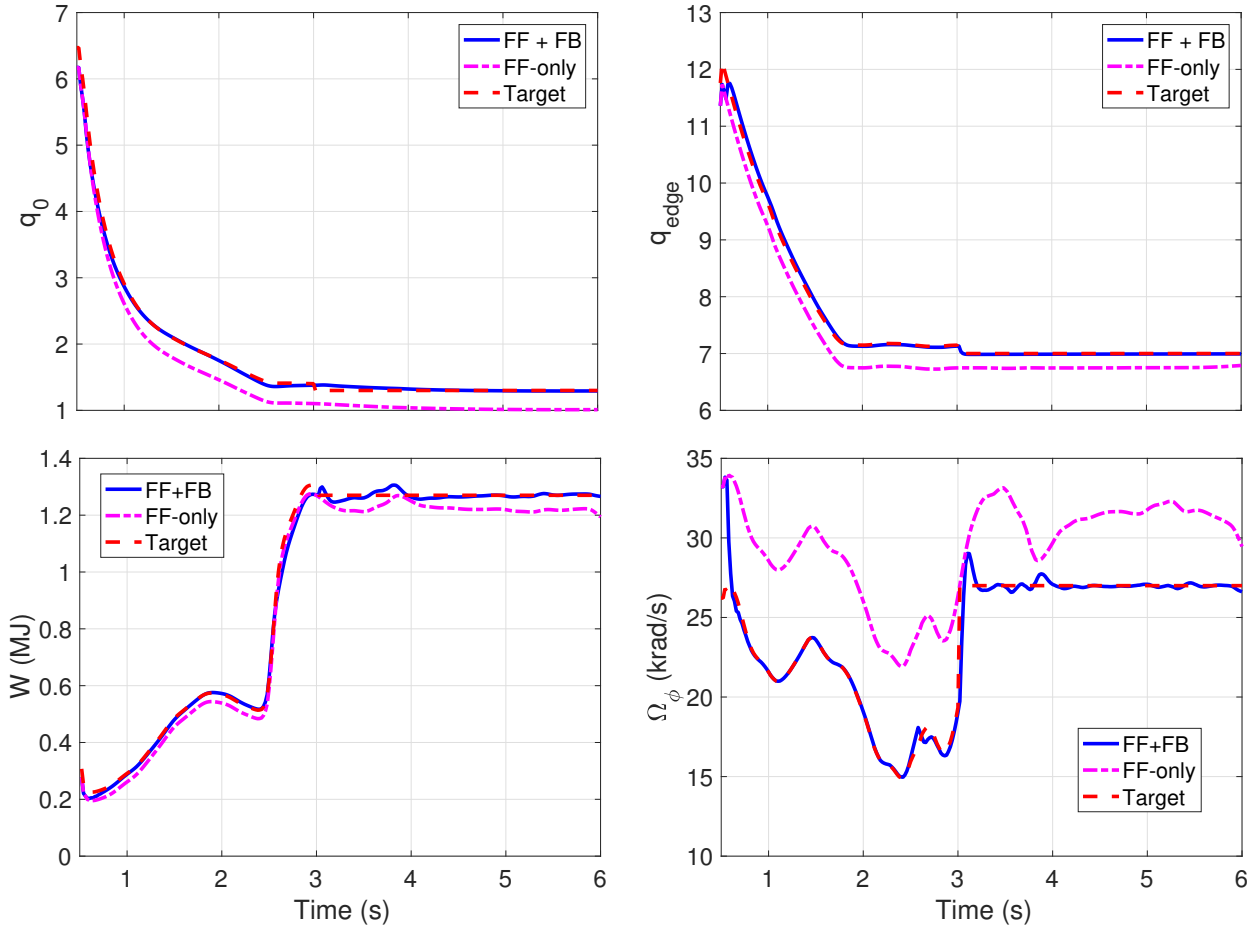

Fig. 2. Comparison of time evolutions for q_0, q_{edge}, W, and Ω_ϕ in 1D simulations.

E. Determination of u by means of optimization

The four equations obtained for the control laws define constraints for the components of u, i.e.,

$$I_p = I_p^{nom} + I_p^{rob}, \tag{35}$$

$$\sum_{i=1}^{N_{NBI}} P_{NBI,i} + P_{EC} = P_{tot}^{nom} + P_{tot}^{rob}, \tag{36}$$

$$\sum_{i=1}^{N_{NBI}} k_{NBI,i} P_{NBI,i} = T_{NBI}^{nom} + T_{NBI}^{rob}, \tag{37}$$

$$F[P_{NBI,1}, ..., P_{NBI,N_{NBI}}, P_{EC}] = F(P^{nom} + P^{rob}), \tag{38}$$

where I_p^{nom}, I_p^{rob}, P_{tot}^{nom}, P_{tot}^{rob}, T_{NBI}^{nom}, T_{NBI}^{rob}, P^{nom} and P^{rob} are determined from (21), (23)-(24), (25), (26)-(27), (28), (29)-(30), (32), and (33)-(34), respectively. The system (35)-(38) has 4 equations with $N_{NBI}+2$ unknowns ($P_{NBI,i}$ for $i = 1, ..., N_{NBI}$, P_{EC}, and I_p). If $N_{NBI} > 2$, then (35)-(38) is an underconstrained system, and additional constraints must be added to univocally determine the components of u. For example, the DIII-D tokamak has 8 NBIs whose powers can be controlled independently, so $N_{NBI}=8$.

A possible way to solve (35)-(38) is to write it as an optimization problem, in which a cost function $J = J(u)$ has to be minimized or maximized in u and subject to the constraints (35)-(38). Additional constraints can be added to the optimization scheme, such as the physical actuation limits existing on u. In this work, $J = u_{FB}^T Q u_{FB}$ is minimized, where $u_{FB} \triangleq u - u^{ref}$ is the feedback input, u^{ref} is a reference input, and Q is a design matrix.

IV. Simulation Study

In this section, the control algorithm previously introduced is tested in 1D simulations using the COTSIM code for a DIII-D scenario. The simulation study is carried out for DIII-D shot 147634. Saturation limits are employed for $P_{NBI,i}, P_{EC} \in [0, 3]$ MW. COTSIM is a 1D code for control testing and simulation that evolves ψ, T_e, and ω_ϕ using the MDE (6) together with the electron heat-transport equation (EHTE) and the toroidal rotation (TRE) equation, which are given by

$$\frac{\partial(\frac{3}{2} n_e T_e)}{\partial t} = \frac{1}{\rho_b^2 \hat{\rho} \hat{H}} \frac{\partial}{\partial \hat{\rho}} \left(\hat{\rho} \frac{\hat{G}\hat{H}^2}{\hat{F}} \chi_e n_e \frac{\partial T_e}{\partial \hat{\rho}} \right) + Q_e, \tag{39}$$

$$m_i \langle r^2 \rangle \frac{\partial(n_i \omega_\phi)}{\partial t} = \frac{1}{\hat{\rho}\hat{H}} \frac{\partial}{\partial \hat{\rho}} \left(f_\phi \chi_\phi n_i \frac{\partial \omega_\phi}{\partial \hat{\rho}} \right) + t_\omega, \tag{40}$$

where χ_e and χ_ϕ are the electron heat and toroidal momentum diffusivities, respectively, m_i is the ion mass, Q_e and t_ω are the electron-heat and ion-torque depositions, respectively, and $\langle r^2 \rangle$ and f_ϕ are profiles corresponding to a particular magnetic configuration. Control-oriented models are used for n_e, n_i, j_{ni}, Q_e, and t_ω, and a Spitzer-like model is used for η. It also employs a mixed Bohm/Gyro-Bohm model [14] for

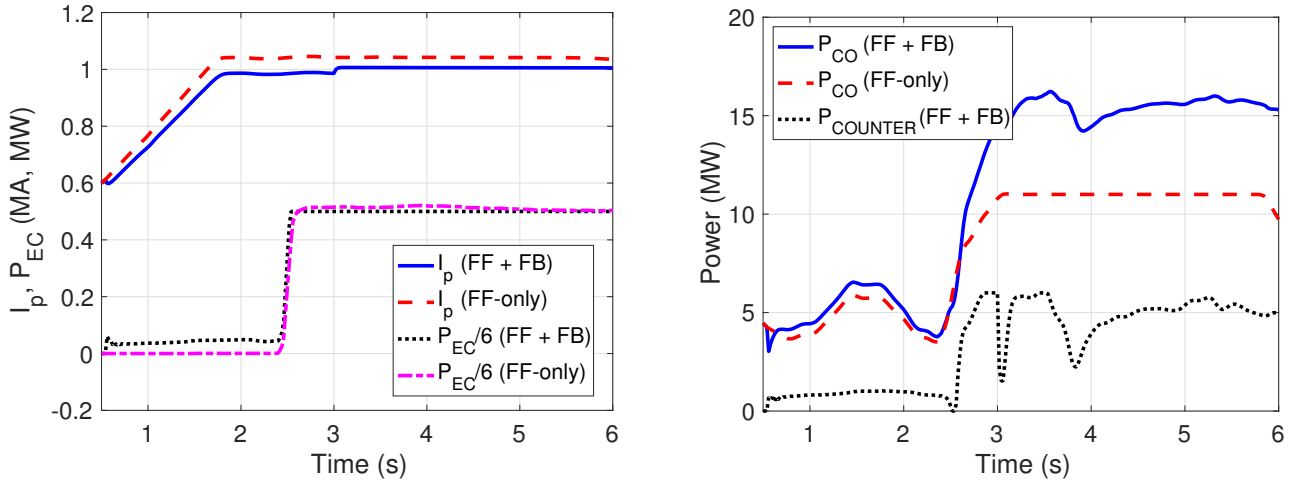

Fig. 3. Comparison of time evolutions for I_p, P_{EC}, co-current NBI power, P_{CO}, and counter-current NBI power, $P_{COUNTER}$.

χ_e and χ_ϕ, which are functions of q among other variables. Therefore, the MDE, EHTE, and TRE are coupled by means of both their diffusive terms (through η, χ_e, and χ_ϕ) and their source terms (through j_{ni}, Q_e, and t_ω).

First, a feedforward-only (FF) simulation is carried out in COTSIM with the inputs u^{ref} corresponding to shot 147634, which is employed as the reference. The state evolution is denoted by x^{ref}. A target $\bar{x}$ is created as a modification of this simulated reference discharge, so that $\bar{q}_{edge} = q_{edge}^{ref} + 0.4$, $\bar{W} = W^{ref} + 0.03$ MJ, $\bar{q}_0 = q_0^{ref} + 0.3$, and $\bar{\Omega}_\phi = \Omega_\phi^{ref} - 7$ krad/s from the beginning of the simulation until $t = 3$ s, whereas from $t = 3$s until the end of the simulation the targets are kept fixed, $\bar{q}_{edge} = 7$, $\bar{W} = 1.27$ MJ, $\bar{q}_0 = 1.3$, and $\bar{\Omega}_\phi = 27$ krad/s . Second, a closed-loop simulation (feedforward + feedback, FF + FB) is run in which the controller tries to drive the system to the target $\bar{x}$. Fig. 2 shows the state evolution for both the FF and FF + FB simulations, together with the target $\bar{x}$. Fig. 3 shows the I_p, P_{EC} evolutions, co-current NBI power, P_{CO} (it includes 6 NBI's), and counter-current NBI power, $P_{COUNTER}$ (it includes 2 NBI's), both in FF and FF + FB simulations ($P_{COUNTER}$ is not shown for the FF simulation because it is constantly zero). It can be seen that the nominal controller successfully drives x to the target $\bar{x}$. All powers and I_p are initially increased to achieve the higher $\bar{q}_{edge}$ and $\bar{W}$ required. Also, P_{CO} is initially reduced whereas $P_{COUNTER}$ is initially increased to spin down the plasma and achieve the lower $\bar{\Omega}_\phi$ required. Moreover, due to the increase in P_{EC}, and probably also due to the increases in P_{tot} and W (and therefore, a decrease in η), q_0 increases as well. At $t = 3$ s, sudden control actions in I_p and $P_{COUNTER}$ are found to drive q_{edge} and Ω_ϕ to their targets. The state x is successfully driven to $\bar{x}$ after $t = 3$ s as well.

V. Conclusions and Future Work

A robust controller for the simultaneous regulation of the central safety factor, edge safety factor, stored energy and toroidal rotation in tokamaks has been presented. It is a model-based controller synthesized from nonlinear, control-oriented models of the 0D dynamics of such individual scalars. Its embedded optimization scheme is highly configurable by means of the design matrix Q, which defines the optimization problem and, therefore, the optimal control actions. Moreover, the controller shows promising results in 1D simulations using COTSIM. Future work may include experimental testing of the control algorithm in DIII-D.

References

[1] J. Wesson, *Tokamaks*. Oxford, UK: Clarendon Press, 1984.

[2] J. T. Scoville and others, "Simultaneous feedback control of plasma rotation and stored energy on the DIII-D tokamak," *Fusion Engineering and Design*, vol. 82, no. 5-14, pp. 1045–1050, 2007.

[3] W. P. Wehner, J.E. Barton and E. Schuster, "Combined rotation profile and plasma stored energy control for the DIII-D tokamak via MPC," in *American Control Conference*, 2017, pp. 4872–4877.

[4] I. R. Goumiri *et al.*, "Simultaneous feedback control of plasma rotation and stored energy on NSTX-U using neoclassical toroidal viscosity and neutral beam injection," *Phys. Plasmas*, vol. 24, no. 056101, 2017.

[5] J. Barton, W. Wehner, E. Schuster, F. Felici, and O. Sauter, "Simultaneous closed-loop control of the current profile and the electron temperature profile in the TCV tokamak," in *American Control Conference*, 2015, pp. 3316–3321.

[6] W. Wehner *et al.*, "Predictive control of the tokamak q profile to facilitate reproducibility of high-$q_{\min}$ steady-state scenarios at DIII-D," in *IEEE Conference on Control Applications*, 2016, pp. 629–634.

[7] W. Shi, W. Wehner, J. Barton *et al.*, "System identification and robust control of the plasma rotational transform profile and normalized beta dynamics for advanced tokamak scenarios in DIII-D," *Fusion Engineering and Design*, vol. 117, pp. 39–57, 2017.

[8] W. P. Wehner *et al.*, "Optimal current profile control for enhanced repeatability of L-mode and H-mode discharges in DIII-D," *Fusion Engineering and Design*, vol. 123, pp. 513–517, 2017.

[9] F. Hinton and R. Hazeltine, "Theory of plasma transport in toroidal confinement systems," *Rev. Mod. Phys.*, vol. 48, pp. 239–308, 1976.

[10] A. Pajares and E. Schuster, "Nonlinear robust safety factor profile control in tokamaks via feedback linearization and nonlinear damping techniques," in *IEEE Conference on Control Applications*, 2018, pp. 306–311.

[11] N. A. Uckan, "Confinement capability of ITER-EDA design," *Proceedings of the 15th IEEE/NPSS Symposium on Fusion Engineering*, vol. 1, pp. 183–186, 1993.

[12] A. Pajares and E. Schuster, "Integrated robust control of the global toroidal rotation and total plasma energy in tokamaks," *IEEE Transactions on Plasma Science*, 2019, under review.

[13] H. Khalil, *Nonlinear Systems*, 3rd ed. New Jersey: Prentice Hall, 2001.

[14] M. Erba *et al.*, "Validation of a new mixed Bohm/gyro-Bohm model for electron and ion heat transport against the ITER, Tore Supra and START database discharges," *Nuclear Fusion*, vol. 38, no. 7, pp. 1013–1028, 1998.